Kinetics of the Reaction between Acetylperoxy and Ethylperoxy Radicals

M. Matti Maricq* and Joseph J. Szente

Research Laboratory, Ford Motor Company, P.O. Box 2053, Drop 3083, Dearborn, Michigan 48121

Received: August 27, 1999; In Final Form: May 22, 2000

Time-resolved ultraviolet (UV) spectroscopy is used to investigate the reaction between $CH_3C(O)O_2$ and $C_2H_5O_2$ at 130 Torr total pressure and over the 220−440-K temperature range. Deconvolution of the UV spectra yields concentration versus time profiles for the acetylperoxy radical and for the $C_2H_5O_2 + CH_3O_2$ composite. The analysis of these data over short times, during which $CH_3C(O)O_2$ radicals are present, yields a temperature-dependent rate constant of $k_1 = (5^{+5}_{-2}) \times 10^{-13}e^{(1070 \pm 200)/T}$ cm^3 s^{-1} for the title reaction. The subsequent long-time decay of the ethylperoxy radicals that remain, after the reaction with $CH_3C(O)O_2$ is complete, is faster than when acetaldehyde and, therefore, acetylperoxy radicals are not present. The secondary chemistry that potentially contributes to this decay is discussed.

I. Introduction

The acetylperoxy radical is an important intermediate in the atmospheric formation and loss of peroxyacetyl nitrate (PAN). The radical is generated during the photochemically initiated oxidation of a variety of carbonyl precursors that originate from both anthropogenic and biogenic emissions. PAN represents a central component of smog. It serves as a temporary reservoir for NO_x, allowing this pollutant to be transported over long distances, for example, from urban to rural areas.

Recently, Stockwell et al.[1] examined the effect that acetylperoxy−peroxy radical reactions might have on PAN and ozone concentrations. The impetus for this modeling study was to investigate possible explanations of field observations that nighttime PAN concentrations fall more rapidly than those of ozone.[2,3] The authors concluded that acetylperoxy−peroxy radical reactions are important at night. This conclusion was echoed by Villenave et al.[4] By measuring a variety of $CH_3C(O)O_2 + RO_2$ room-temperature rate constants, they ascribed a generic value of 1×10^{-11} cm^3 s^{-1} to the rate constant for this class of reactions, and found that its contribution to the atmospheric chemistry of acetylperoxy radicals and PAN could not be neglected.

Despite these findings, there are few detailed kinetic studies of reactions representative of the acetylperoxy−peroxy class. Temperature-dependent rate constants have been measured for the $CH_3C(O)O_2$ self-reaction and for its cross reaction with CH_3O_2 by Moortgat et al.[5] and by Maricq and Szente,[6] and for the $CH_3C(O)O_2 + HO_2$ reaction by Moortgat et al.[7] and Crawford et al.[8] Room-temperature measurements exist for $CH_3C(O)O_2$ reactions with $C_2H_5O_2$,[9] with $CH_3C(O)CH_2O_2$,[10] and with *c*-$C_6H_{11}O_2$, *sec*-$C_{10}H_{21}O_2$, *sec*-$C_{12}H_{25}O_2$, and *t*-$C_4H_9O_2$.[4] Except for the results of Bridier et al.,[10] all of the room-temperature rate constants equal 1×10^{-11} cm^3 s^{-1} within an experimental error of about ± 0.3.

The paucity of kinetic data for these peroxy radical−radical reactions is at least partly due to the difficulty in making such measurements. The acetylperoxy radical reacts rapidly with itself and produces methylperoxy radicals as a secondary species, thereby complicating kinetic analyses. In the present work, the ethylperoxy radical is chosen as the reaction partner because its self-reaction is both slow and well characterized. Also, time-resolved ultraviolet (UV) spectroscopy is used record time and wavelength-resolved absorption profiles of the reaction mixture to help distinguish the decays of the acetylperoxy and ethylperoxy concentrations as the reaction proceeds. Despite these efforts, secondary chemistry is found to have an important influence, and the long-time decay of the ethylperoxy radicals that remain after the acetylperoxy radicals have been depleted cannot be adequately described within the existing kinetic model. Fortunately, these secondary complications arise on a time scale that is long compared with the lifetime of $CH_3C(O)O_2$ radicals; therefore, by focusing on the short-time kinetic profiles, the $CH_3C(O)O_2 + C_2H_5O_2$ rate constant can measured with an acceptably small error arising from uncertainties in the secondary chemistry.

II. Experimental Section

The flash photolysis−time-resolved UV spectroscopy technique used for the present experiments was the same as applied in our previous studies of acetylperoxy kinetics; thus, only a brief description of the apparatus is given here, and the reader is directed to refs 6, 8, and 11 for a more complete description. The reactor consisted of a 53-cm long, 3.5-cm diameter, Pyrex cylinder. Light from an eximer laser was collimated from its normal rectangular beam profile to a ∼1.5-cm square geometry, using cylindrical optics, and directed coaxially through the cell. A 10-ns, ∼300-mJ, pulse of 351-nm light initiated the radical chemistry by dissociating a fraction of the Cl_2 molecules in a slowly flowing $CH_3CHO/C_2H_6/Cl_2/O_2/N_2$ gas mixture (total flow = 2.5 Standard liters per minute (SLPM) concentrations are given in Table 2) to generate $(4-10) \times 10^{14}$ chlorine atoms/cm^3 within the irradiated volume. By choosing ≳ 2 Torr of organic precursor and ≳ 20 Torr O_2, the Cl atoms are nearly

* Author for correspondence.

10.1021/jp9930649 CCC: $19.00
Published on Web 07/14/2000

quantitatively converted within a few microseconds to the starting peroxy radicals via the following reactions:

$$Cl + CH_3CHO \rightarrow CH_3CO + HCl \quad (1)$$

$$CH_3CO + O_2 + M \rightarrow CH_3C(O)O_2 + M \quad (2)$$

$$Cl + C_2H_6 \rightarrow C_2H_5 + HCl \quad (3)$$

$$C_2H_5 + O_2 + M \rightarrow C_2H_5O_2 + M \quad (4)$$

The total initial radical concentration was confirmed in companion measurements of the ethylperoxy radicals formed in the absence of acetaldehyde.[11] Because the ethylperoxy radicals decayed only on the millisecond time scale, their concentration was easily extrapolated to zero time and equated with $[Cl]_0$.

Following their initial formation, the $CH_3C(O)O_2$ and $C_2H_5O_2$ concentrations were monitored as a function of the time by UV spectroscopy. The probe UV light was provided by a deuterium lamp. It was collimated, apertured to 0.9 cm, and overlayed collinearly with the central portion of the photolysis beam. Restricting the probe beam diameter limits it to a region with approximately uniform Cl atom concentration and provides a buffer region where radicals are formed, but are not probed, thereby reducing the loss of radicals by diffusion from the field of view. The actual, nonchemical, loss of radicals from the probe volume occurs because of both diffusion and the flow of the reaction mixture out of the cell. Experimental measurement of this composite loss rate was achieved by replacing the ethane and acetaldehyde precursors with toluene, under otherwise similar conditions. The photolysis of Cl_2 then produced benzylperoxy radicals and, subsequently, the stable product benzaldehyde. The strong UV absorption by benzaldehyde exhibited an essentially exponential decay, with a half-life of ~800 ms. Thus, the losses by diffusion and by pumping of the reaction mixture through the cell remain <10% for times <125 ms.

The probe light was dispersed at a resolution of ~2 nm with a 0.32-m monochromator (SA HR 320) and detected with a gated diode array detector, with an intensifier optimized for the UV range (Princeton Instruments IPDA-700SB with ST1000 controller). Although the intensifier has a gain of $>10^5$, the probe light could "leak" through the intensifier and accumulate charge on the diodes during the time between photolysis pulses, an effect that increases as λ decreases. To avoid this interference, a mechanical shutter was placed in front of the monochromator that opens only when the photolysis is triggered. At each delay time after photolysis, ranging from 10 μs to 25 ms, three spectra were taken at 20-ms intervals, each with a gate time of 10−20 μs. The first spectrum "cleans" the diode array by reading the array and resetting it. (This further reduces the effect of the leakage light and removes dark current that might have accumulated on the diodes. The result is a gate-on/gate-off ratio of >1000 for most of the UV range and >100 for λ < 215 nm.) The second spectrum precedes the laser photolysis pulse to provide I_0 for Beer's Law. The third spectrum follows the photolysis pulse by the selected delay time to measure I_t, the transmitted intensity at time t. The UV spectra collected in this way were typically averaged over 500−750 photolysis pulses. The laser repetition rate was 2 Hz, implying ~3 flashes during the ~1.5 s required for the gases to flow through the cell. Checks showed that spectra obtained at lower repetition rates do not differ significantly from those obtained at 2 Hz.

In general, the net absorbance consists of a number of broad superimposed spectra originating from the various UV absorbing species generated in the reaction mixture. In the present experiments, these species include the principal reactants, $CH_3C(O)O_2$ and $C_2H_5O_2$, secondary CH_3O_2 radicals produced by the acetylperoxy self-reaction, and "products", which are a collection of weakly absorbing stable species, such as C_2H_5OOH, that are produced as a result of the photooxidation of acetaldehyde and ethane. In principle, HO_2 is also formed as a secondary species, but in these experiments its concentration remains too low (≲5% of the radical concentration) to merit consideration. Thus, the reaction mixture absorbances are deconvoluted according to the expression

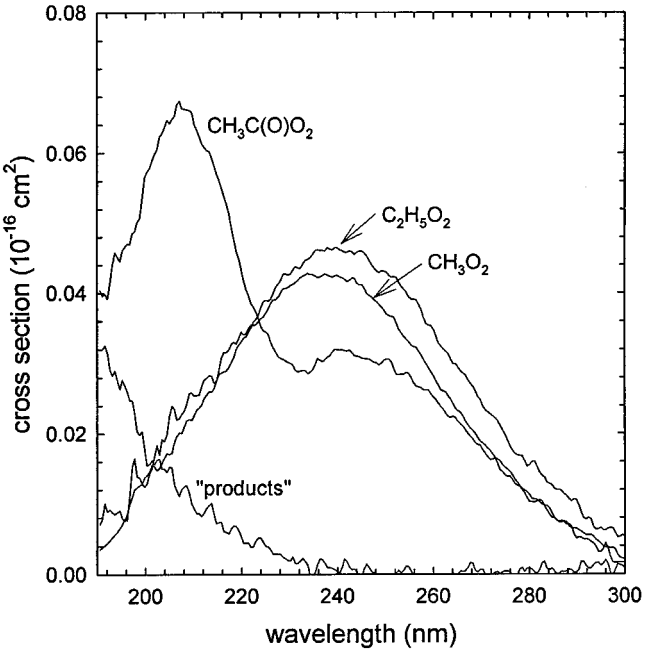

Figure 1. UV reference spectra of the principal species contributing to the time-resolved absorbance spectra for the $CH_3C(O)O_2 + C_2H_5O_2$ reaction mixture. Reference spectra are obtained as follows: $CH_3C(O)O_2$ (ref 6), $C_2H_5O_2$, (ref 11), CH_3O_2 (ref 11), and "products" (present work).

$$\mathrm{Abs}(t) = \Sigma\,[x_i]_t \sigma(x_i) l \quad (5)$$

where l represents the path length (53 cm), σ is the absorption cross section, $[x]_t$ is the concentration at delay time t, and the index $i = 1-4$ accounts for the contributions of acetylperoxy, ethylperoxy, methylperoxy, and "products" to the overall absorbance. The relevant reference spectra are illustrated in Figure 1; the reference spectrum for "products" is the residual UV absorption recorded at 20 ms, after reaction of the peroxy radicals is complete. It is not the point here to quantify the amount of "products". Rather, this absorbance is included in the fitting procedure to improve the accuracy in determining the acetylperoxy and ethylperoxy concentrations; that is, if "products" were not included in the fit, the presence of these species in the reaction mixture would lead to an overestimate of acetylperoxy radicals.

The experiments were conducted over the 220−440 K temperature range. In most cases, the temperature was controlled (to within 5 K) by a recirculating chiller (Neslab ULT-80dd) that flows methanol or ethylene glycol through a jacket surrounding the reactor. The data at 333, 395, and 435 K were taken using a new, high-temperature quartz cell (of similar dimensions) that is electrically heated. The gases were precooled/preheated prior to entering the cell, resulting in a temperature profile that was uniform over 90% of the reactor length; at the entrance it fell off by 20 K (at 220 and 360 K, less as 295 K is approached) over the first 5 cm. Acetaldehyde

TABLE 1: $CH_3C(O)O_2 + C_2H_5O_2$ Reaction Mechanism

reaction	rate constant[a]
principal	
6a. $CH_3C(O)O_2 + C_2H_5O_2 \rightarrow CH_3C(O)O + C_2H_5O + O_2$	$k_6 = 5 \times 10^{-13}\, e^{1070/T}\ cm^3\ s^{-1}$[b]
6b. $CH_3C(O)O_2 + C_2H_5O_2 \rightarrow CH_3COOH + CH_3CHO + O_2$	$k_{6b}/k_6 = 0 - 0.2$[b]
7. $CH_3C(O)O_2 + CH_3C(O)O_2 \rightarrow 2\ CH_3C(O)O + O_2$	$k_7 = 3.0 \times 10^{-12}\, e^{504/T}\ cm^3\ s^{-1}$ (ref 6)
8a. $C_2H_5O_2 + C_2H_5O_2 \rightarrow 2\ C_2H_5O + O_2$	$k_8 = 9.8 \times 10^{-14} \exp(-100/T)\ cm^3\ s^{-1}$
8b. $C_2H_5O_2 + C_2H_5O_2 \rightarrow C_2H_5OH + CH_3CHO + O_2$	$k_{8b}/k_8 = 0.35$
secondary	
9. $CH_3C(O)O \rightarrow CH_3 + CO_2$	$k_9 > 1 \times 10^6\ s^{-1}$
10. $CH_3 + O_2 + M \rightarrow CH_3O_2 + M$	$k_{10} = 4.5 \times 10^{-31}\, (T/300)^{-3}\ cm^6\ s^{-1}$
$CH_3C(O)O_2 + CH_3O_2 \rightarrow CH_3C(O)O + CH_3O + O_2$	$k = 0\ cm^3\ s^{-1}$ (ref 6)
$CH_3C(O)O_2 + CH_3O_2 \rightarrow CH_3COOH + CH_2O + O_2$	$k = 8.5 \times 10^{-13}\, e^{726/T}\ cm^3\ s^{-1}$ (ref 6)
$C_2H_5O_2 + CH_3O_2 \rightarrow C_2H_5O + CH_3O + O_2$	$k = 1 \times 10^{-13}\ cm^3\ s^{-1}$ (ref 9)
$C_2H_5O_2 + CH_3O_2 \rightarrow$ other products	$k = 1 \times 10^{-13}\ cm^3\ s^{-1}$ (ref 9)
tertiary	
$CH_3O_2 + CH_3O_2 \rightarrow 2\ CH_3O + O_2$	$k = (1 - b) \times 9.1 \times 10^{-14} e^{416/T}\ cm^3\ s^{-1}$
$CH_3O_2 + CH_3O_2 \rightarrow CH_3OH + CH_2O + O_2$	$k = b \times 9.1 \times 10^{-14}\, e^{416/T}\ cm^3\ s^{-1}$
	$b = (1 + 25 \times e^{-1165/T})^{-1}$
$C_2H_5O + O_2 \rightarrow CH_3CHO + HO_2$	$k = 1.0 \times 10^{-13}\, e^{-830/T}\ cm^3\ s^{-1}$
$CH_3O + O_2 \rightarrow CH_2O + HO_2$	$k = 3.9 \times 10^{-14}\, e^{-900/T}\ cm^3\ s^{-1}$
$RO_2 + RO \rightarrow RH_{-1}O + ROOH$	$k = 1.5 \times 10^{-12}\ cm^3\ s^{-1}$
$RO + RO \rightarrow RH_{-1}O + ROH$	$k = 3 \times 10^{-11}\ cm^3\ s^{-1}$
$C_2H_5O_2 + HO_2 \rightarrow C_2H_5OOH + O_2$	$k = 6.9 \times 10^{-13}\, e^{(702/T)}\ cm^3\ s^{-1}$
$CH_3O_2 + HO_2 \rightarrow CH_3OOH + O_2$	$k = 4.1 \times 10^{-13}\, e^{(790/T)}\ cm^3\ s^{-1}$
$CH_3C(O)O_2 + HO_2 \rightarrow$ products	$k = 3.9 \times 10^{-13}\, e^{(1350/T)}\ cm^3\ s^{-1}$ (ref 8)
$HO_2 + HO_2 \rightarrow HOOH + O_2$	$k = 2.8 \times 10^{-13}\, e^{(594/T)}\ cm^3\ s^{-1}$
$HO_2 + CH_3CHO \rightarrow CH_3C(OH)HO_2$	$k = 5 \times 10^{-14}\ cm^3\ s^{-1}$ (ref 8)
$CH_3O + CH_3CHO \rightarrow CH_3CO + CH_3OH$	$k = 7 \times 10^{-14}\ cm^3\ s^{-1}$ (ref 14)
$C_2H_5O + CH_3CHO \rightarrow CH_3CO + C_2H_5OH$	$k = (5 - 50) \times 10^{-15}\ cm^3\ s^{-1}$

[a] Rate constants taken from refs 12 and 13 unless otherwise noted. [b] Measured in the present study.

(99%) was obtained from Fisher, chlorine (4.8% in nitrogen) was from Matheson, and ethane (99.5%), oxygen (ultrazero grade), and nitrogen (99.999%) were from Michigan Airgas. Tylan flow controllers maintained flows of all the gases except chlorine, which was regulated with a needle valve.

III. Results

The reactant peroxy radicals are formed essentially instantly (~1 μs) compared with the 100−300-μs time scale of their subsequent chemistry. Therefore, the primary reactions responsible for the observed evolution in UV absorbance with time include

$$CH_3C(O)O_2 + C_2H_5O_2 \rightarrow CH_3C(O)O + C_2H_5O + O_2 \quad (6a)$$

$$CH_3C(O)O_2 + C_2H_5O_2 \rightarrow CH_3COOH + CH_3CHO + O_2 \quad (6b)$$

$$CH_3C(O)O_2 + CH_3C(O)O_2 \rightarrow 2\ CH_3C(O)O + O_2 \quad (7)$$

$$C_2H_5O_2 + C_2H_5O_2 \rightarrow 2\ C_2H_5O + O_2 \quad (8a)$$

$$C_2H_5O_2 + C_2H_5O_2 \rightarrow C_2H_5OH + CH_3CHO + O_2 \quad (8b)$$

The full reaction model is presented in Table 1 (unless otherwise noted, peroxy radical rate constants were taken from ref 12, whereas the remainder were from ref 13).

The primary reactions qualitatively explain the changes observed in the time-resolved spectra displayed in Figure 2, which represents the raw data from which the rate constant determinations are made. The bimodal pattern observed near $t = 0$ corresponds to a nearly equal mixture of acetylperoxy radicals, which have absorption peaks at 207 and 242 nm, and ethylperoxy radicals, which exhibit an absorption maximum at 239 nm (see Figure 1). The short wavelength feature decays within ~200 μs, indicating the loss of acetylperoxy radicals; however, after an initial rapid decay, the 240-nm feature decays only on a much slower time scale. This result is consistent with UV absorption by ethylperoxy radicals that remains after completion of reactions 6 and 7, and is only slowly removed by reaction 8.

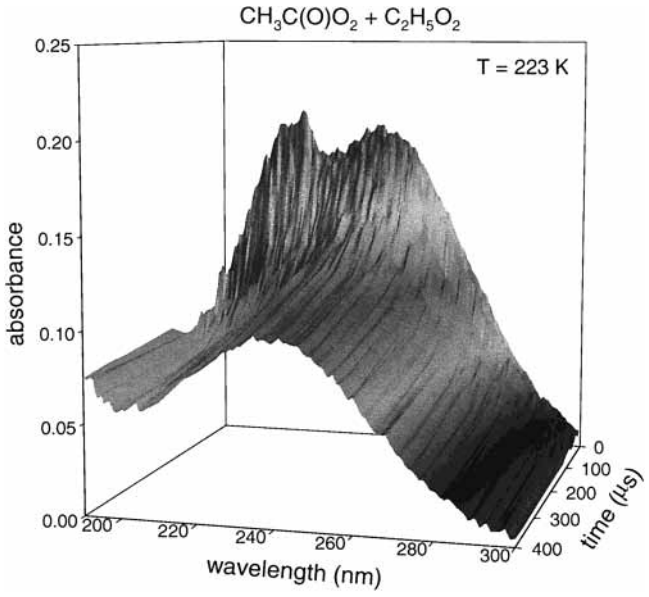

Figure 2. UV absorbance of the reaction mixture as a function of wavelength and time after photolysis.

This simple picture must be amended for the secondary radicals produced via reactions 6a, 7, and 8a. Most important are the $CH_3C(O)O$ radicals formed in reactions 6a and 7 because they are unstable with respect to dissociation and rapidly convert to methylperoxy radicals via

$$CH_3C(O)O \rightarrow CH_3 + CO_2 \quad (9)$$

$$CH_3 + O_2 + M \rightarrow CH_3O_2 + M \quad (10)$$

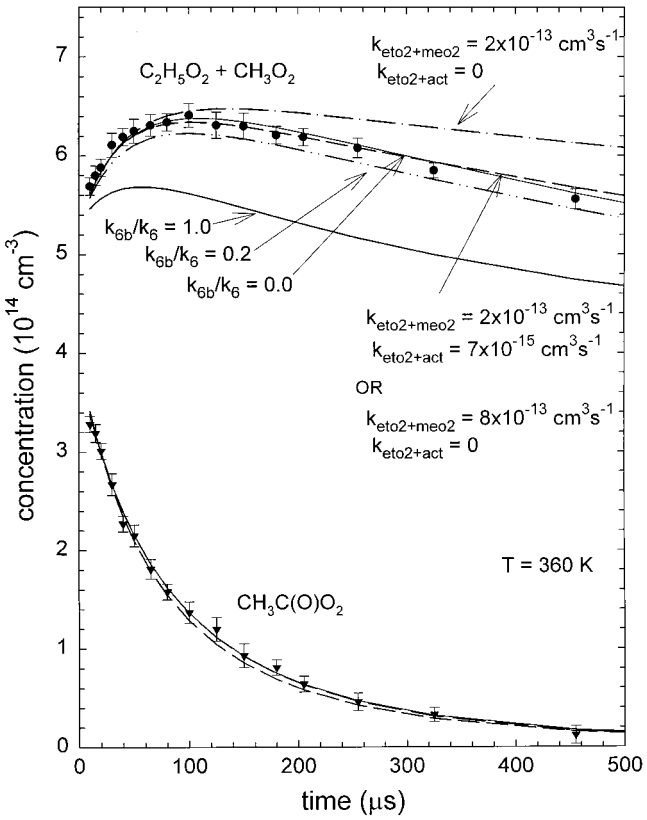

Figure 3. Concentration versus time profiles for $CH_3C(O)O_2$ and $RO_2 = C_2H_5O_2 + CH_3O_2$, as determined from the deconvolution of time-resolved UV absorbance data, such as illustrated in Figure 2. Symbols denote the experimental data. The lines illustrate fits to the reaction model assuming the acetylperoxy + ethylperoxy reaction to proceed via the radical (6a) versus molecular (6b) channel (at $k_{6b}/k_6 = 0$, 0.2, and 1) and assuming the existence versus absence of secondary ethylperoxy removal.

CH_3O_2 poses two problems with respect to the present study: it reacts with acetylperoxy and ethylperoxy radicals, but moreover, its UV absorption spectrum is nearly identical to that of ethylperoxy (see Figure 1). Thus, in reality, our spectral deconvolution (eq 5) provides the summed $C_2H_5O_2 + CH_3O_2$ concentration, not that of $C_2H_5O_2$ itself. Because the kinetics of the $CH_3C(O)O_2 + CH_3O_2$ reaction is relatively well established (although the product branching ratio remains in question[5,6]) and the ethylperoxy concentration typically exceeds that of methylperoxy by a factor of 1.5−2, the interference between these two peroxy radicals introduces only a modest uncertainty into the determination of k_6.

The effects of the secondary methylperoxy radicals are immediately apparent in Figure 3. This plot illustrates the $CH_3C(O)O_2$ and the $C_2H_5O_2 + CH_3O_2$ composite concentration versus time profiles that are extracted from deconvoluting time-resolved UV absorbance spectra, such as those in Figure 2. Although one expects from the primary peroxy chemistry (reactions 6−8) that both the acetylperoxy and composite alkylperoxy concentrations decrease with time, the experimental measurements show the $C_2H_5O_2 + CH_3O_2$ concentration to increase at first, due to the secondary methylperoxy formation, and then slowly decrease. This initial increase cannot be accounted for simply by the methylperoxy radicals formed as a result of the acetylperoxy self-reaction, as illustrated by the curve marked $k_{6b}/k_6 = 1$ in Figure 3. Instead, for all of the experimental measurements listed in Table 2, the $C_2H_5O_2 + CH_3O_2$ concentration data can only be fit by setting $k_{6b}/k_6 = 0$; that is, having the reaction proceed entirely via the radical channel. For the example in Figure 3, varying the branching fraction k_{6b}/k_6 within the range 0.0−0.2 provides an acceptable fit within the 2σ errors in the $C_2H_5O_2 + CH_3O_2$ composite concentration measurements; thus, this interval effectively provides the 2σ, or 95%, confidence interval for k_{6b}/k_6. As noted in Table 2, this range applies to the majority of experimental measurements, although the confidence interval increases to 0.0−0.3 and 0.0−0.4 at the ends of the temperature range covered by the present experiments. Note also that the choice of branching ratio affects primarily the $C_2H_5O_2 + CH_3O_2$ composite concentration. It has only a minor effect on the $CH_3C(O)O_2$ concentration because the acetylperoxy radicals decay primarily due to their self-reaction and reaction with $C_2H_5O_2$, and less as a result of the cross reaction with secondary CH_3O_2 radicals.

On setting $k_{6b}/k_6 = 0$, the decay in $CH_3C(O)O_2$ and the initial rise in $C_2H_5O_2 + CH_3O_2$ concentrations are satisfactorily explained by reactions 6−10 (and the $CH_3C(O)O_2 + CH_3O_2$ reaction). However, the observed long-term decay in $C_2H_5O_2 + CH_3O_2$ concentration is faster than expected from the simple model, as indicated by the dot−dash curve at the top of Figure 3, even after accounting for the cross reaction between ethylperoxy and methylperoxy radicals. A variety of mechanisms can be hypothesized to explain the more rapid than expected decay, as discussed later, and each mechanism improves the agreement between the model predictions and experimental *long-time decay* of the $C_2H_5O_2 + CH_3O_2$ composite concentration. However, knowing the precise nature of the mechanism responsible for this slow decay (out to 25 ms) is not necessary to extract a meaningful rate constant for the acetylperoxy reaction with ethylperoxy.

Before proceeding with the rate constant determinations for the title reaction, we take a closer look at the long-time decay data. Figure 4 expands the time scale of the $C_2H_5O_2 + CH_3O_2$ decay 50-fold, well past the time that the acetylperoxy concentration has decayed to zero. Three sets of data are compared, with the initial acetylperoxy concentrations set at 0, 0.2×10^{14}, and 2.2×10^{14} cm^{-3}. With no acetaldehyde added to the reaction gas mixture, the decay of $C_2H_5O_2$ (no CH_3O_2 is present) follows the predictions of the model in Table 1; that is, it occurs principally via its self-reaction and removal by secondary HO_2 formed from the ethoxy reaction with O_2. However, even in the presence of a small amount of acetylperoxy radicals, ∼5% versus 95% ethylperoxy, the $C_2H_5O_2 + CH_3O_2$ composite decay occurs at a noticeably faster rate (Figure 4, filled inverted triangles compared with open circles). Because the increase in decay rate is more than can be accounted for by the addition of 0.2×10^{14} cm^{-3} of $CH_3C(O)O_2$, and because it continues long after the $CH_3C(O)O_2$ has disappeared, the increased removal rate must arise from secondary chemistry initiated by the addition of acetaldehyde, and thus acetylperoxy radicals, to the reaction mixture. As more acetaldehyde is added, the long-time $C_2H_5O_2 + CH_3O_2$ loss rate increases.

We have identified two potential mechanisms for the enhanced alkylperoxy decay, neither of which is entirely satisfactory: they are, a reaction between $C_2H_5O_2$ and CH_3CHO, and a more rapid than previously reported[9] reaction between $C_2H_5O_2$ and CH_3O_2. Either mechanism can provide excellent fits to the data, both at short times (as illustrated by the solid line fits to the data in Figure 3) and at long times (two examples are given by the curves marked $k_{eto2+meo2} = 13 \times 10^{-13}$ cm^3 s^{-1} in Figure 4). The first mechanism can be tested by varying the amount of acetaldehyde in the initial reaction gas mixture (the ethane level must also be adjusted to keep the initial radical relative concentrations constant). However, a 20-fold increase in CH_3-

TABLE 2: $CH_3C(O)O_2 + C_2H_5O_2$ Rate Constants

temp K	P_{tot} Torr	O_2 Torr	Cl_2 Torr	CH_3CHO Torr	C_2H_6 Torr	$[C_2H_5O_2]_0$ 10^{14} cm^{-3}	$[CH_3C(O)O_2]_0$ 10^{14} cm^{-3}	$k_{CH_3CO_3+C_2H_5O_2}$ 10^{-11} cm^3 s^{-1} [a]	k_{6b}/k_6 range[b]
223	129	28.6	0.26	2.58	3.28	5.1	5.3	4.0 ± 1.7	0−0.3
235	126	27.4	0.21	0.83	2.08	2.6	1.5	4.8 ± 1.6	0−0.3
236	130	28.1	0.22	0.85	2.12	5.9	2.6	4.9 ± 1.5	0−0.3
253	125	27.4	0.18	1.28	3.05	4.2	2.2	3.3 ± 1.7	0−0.2
255	129	28.0	0.23	0.85	2.10	5.4	2.5	4.0 ± 1.9	0−0.2
273	127	27.0	0.26	2.10	2.98	4.8	3.3	2.7 ± 1.0	0−0.2
274	130	28.3	0.23	0.86	2.12	4.9	2.0	3.8 ± 1.1	0−0.2
295	126	27.0	0.30	1.36	3.22	5.1	2.2	2.5 ± 0.8	0−0.2
295	126	27.5	0.21	0.34	0.84	4.3	1.8	2.8 ± 1.2	0−0.3
295	133	28.7	0.21	7.13	17.0	4.6	1.7	1.8 ± 0.8	0−0.3
295	127	27.7	0.22	1.77	2.50	3.8	2.6	1.9 ± 0.7	0−0.4
325	135	28.5	0.32	2.70	3.64	4.9	3.6	1.3 ± 0.4	0−0.2
333	139	28.8	0.30	1.69	3.57	5.3	2.0	1.1 ± 0.4	0−0.2
359	137	28.8	0.36	1.52	3.66	6.1	2.4	1.1 ± 0.5	0−0.2
360	138	28.5	0.32	2.77	3.44	5.3	3.9	0.8 ± 0.15	0−0.2
395	138	30.1	0.33	1.72	3.69	5.8	1.9	0.5 ± 0.3	0−0.4
435	144	31.1	0.37	1.76	3.68	6.9	2.0	0.5 ± 0.3	0−0.3
435	144	128	0.37	1.75	3.65	6.8	2.3	0.9 ± 0.4	0−0.3

[a] Error bars are $\pm 2\sigma$ and include fitting and systematic uncertainties. [b] 2σ confidence interval.

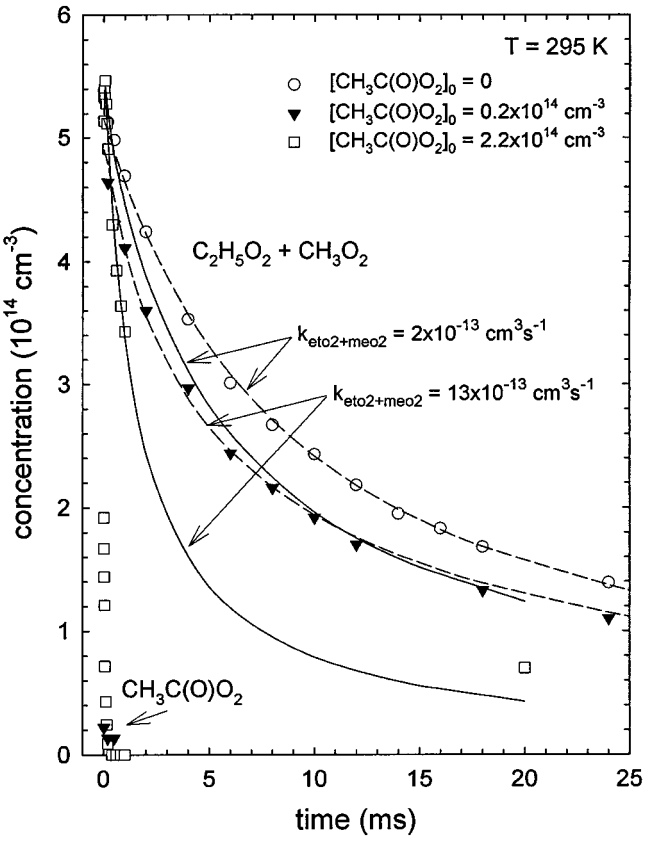

Figure 4. Long-time decay of the ethylperoxy radical for various initial $CH_3C(O)O_2$ concentrations. Note the near instantaneous loss of $CH_3C(O)O_2$ on this time scale. Solid lines show model predictions, comparing two values of $k_{eto2+meo2}$ for the data represented by the open squares; dashed lines are for the inverted triangles. The open circles represent the ethylperoxy decay in the absence of acetaldehyde and, therefore, CH_3O_2.

CHO from 0.34 to 7.1 Torr has a minimal effect on the $C_2H_5O_2 + CH_3O_2$ decay rate (see Table 2), an observation that is inconsistent with the hypothesis that this reaction is responsible for the long-time $C_2H_5O_2 + CH_3O_2$ loss rate.

The second mechanism, increasing the $C_2H_5O_2 + CH_3O_2$ cross reaction rate constant from its reported value[9] of 2×10^{-13} cm^3 s^{-1} to 13×10^{-13} cm^3 s^{-1}, also leads to good agreement with the observed long-time $C_2H_5O_2 + CH_3O_2$ composite decay. Being a radical−radical reaction, this mechanism is independent of the radical precursor concentrations (e.g., acetaldehyde), which is in agreement with experimental results. This mechanism is relatively independent of temperature, as might be expected, with the model-fitted values varying between 8×10^{-13} and 20×10^{-13} cm^3 s^{-1} over the 223−435 K range. Unfortunately, the larger cross reaction rate constant required in the present experiments is inconsistent with peroxy radical decay measurements made in the absence of acetaldehyde and, thus, this mechanism also is not entirely satisfactory.

Another potential complication concerns the fates of the alkoxy radicals that arise from the peroxy chemistry. These can be lost by self-reaction or removed by reaction with peroxy radicals. They can react with O_2 to form HO_2 or with acetaldehyde to regenerate $CH_3C(O)O_2$:

$$RO + CH_3CHO \rightarrow ROH + CH_3CO \qquad (11)$$

The methoxy reaction with acetaldehyde has been reported to occur with a rate constant[14] of 7.4×10^{-14} cm^3 s^{-1}; however, no data are available for the ethoxy case. If the latter reaction is assumed to proceed at the same rate as the methoxy reaction, then it could affect the determination of k_6 (i.e., a factor of 2 change in the rate constant would alter k_6 by ∼20%). However, two observations indicate that $CH_3C(O)O_2$ regeneration would not pose a problem. The first observation is that the best fit values for k_6 do not depend, in a statistically significant way, on the acetaldehyde concentration as it is varied by a factor of 20 (see Table 2). Second, if regeneration is introduced into the model, the fit for k_6 becomes dependent on the length of time after photolysis over which the fit is performed, with k_6 converging to the value found in the absence of regeneration as the time interval is decreased. Both observations suggest that, within the data scatter, complications from the alkoxy chemistry do not affect the measurement of k_6; perhaps the ethoxy reaction with acetaldehyde is slower than the methoxy counterpart or ethoxy radicals are removed by other mechanisms.

Continued exploration of the long-time $C_2H_5O_2 + CH_3O_2$ decay found in the photo-initiated oxidation of acetaldehyde/ethane gas mixtures takes us outside the scope of the present paper. The acetylperoxy decay and the initial rise and early portion of the $C_2H_5O_2 + CH_3O_2$ decay ($t \lesssim 500$ μs) are fit to the reaction model of Table 1 with k_6, $k_{C2H5O2+CH3O2}$ or

$k_{C_2H_5O_2+CH_3CHO}$, $[CH_3C(O)O_2]_0$, and $[C_2H_5O_2]_0$ treated as adjustable parameters, with the latter two subject to the constraint that they sum to the ethylperoxy concentration calibration measurement. The results for k_6, along with the experimental conditions, are listed in Table 2. They are independent, within the experimental error, of whether increasing the ethylperoxy−methylperoxy cross reaction rate constant or a reaction between ethylperoxy and acetaldehyde is used to accommodate the $C_2H_5O_2 + CH_3O_2$ decay.

The error analysis performed for k_6 includes both the "signal noise" originating from the UV absorbances and systematic contributions from uncertainties in the optical cross sections used to deconvolute the absorbances and the rate constants employed in the reaction model used to fit the concentration data. The principal sources of systematic error are $\sigma_{CH_3C(O)O_2}$, $\sigma_{C_2H_5O_2}$, $k_{C_2H_5O_2+CH_3O_2}$ (or $k_{C_2H_5O_2+CH_3CHO}$), k_7, and $k_{CH_3C(O)O_2+CH_3O_2}$. The ethylperoxy self-reaction is too slow for the uncertainty in its rate constant to exert an influence on the determination of k_6. The impact of the first three on the confidence limits for k_6 can be ascertained in two ways.

The first method is via a sensitivity analysis. Thus, modifying the $CH_3C(O)O_2$ concentrations by 10% to account for uncertainty in the acetylperoxy UV cross section alters the best fit value of k_6 by ∼8%. A 5% uncertainty in the better-known ethylperoxy cross section leads to a similar 8% effect on k_6.[11,12] The effect of $k_{C_2H_5O_2+CH_3O_2}$ (or $k_{C_2H_5O_2+CH_3CHO}$) depends on the time interval over which the concentration is fit. The shorter the time interval, the smaller is the effect of either of these rate constants, which are used as surrogates to model the long-time $C_2H_5O_2 + CH_3O_2$ decay. However, shortening the time interval increases the contribution of signal noise to the error in k_6. As a compromise, for the 0−500-μs intervals typically used in the present fits, a 4-fold reduction in $k_{C_2H_5O_2+CH_3O_2}$, essentially reducing it to the previously reported value, has about a 15% effect on the determination of k_6. Uncertainties of the order 10% in the acetylperoxy self-reaction and its cross reaction with methylperoxy lead to errors of 5−10% and ∼4%, respectively, in k_6 (the latter increases to ∼9% at the higher temperatures because of uncertainty in the branching ratio of the cross reaction). When these values are statistically combined with a 15% uncertainty due to "noise", assuming the contributing uncertainties to be independent, the result is the 20−40% error bars reported at 95% confidence in Table 2.

The influence of uncertainties in $\sigma_{CH_3C(O)O_2}$, $\sigma_{C_2H_5O_2}$, and $k_{C_2H_5O_2+CH_3O_2}$ (or $k_{C_2H_5O_2+CH_3CHO}$) can be ascertained in another way. The uncertainties in the cross sections are equivalent to admitting that the initial $CH_3C(O)O_2$ and $C_2H_5O_2$ concentrations are not known and treating these as adjustable model parameters along with the rate constant chosen to model the long-time $C_2H_5O_2 + CH_3O_2$ decay. In addition to the best fit parameters, the fitting software (Scientist, MicroMath Scientific Software) provides a statistical analysis of the parameters, in particular providing both univariate and support plane confidence intervals. The latter allows that the roles played in the model by the various adjustable parameters may be correlated and, thus, provides an ellipsoidal joint confidence region for the four parameters just mentioned. This procedure results in a 15−35% error in k_6, accounting for the effects of varying the other three parameters, namely, $\sigma_{CH_3C(O)O_2}$, $\sigma_{C_2H_5O_2}$, and $k_{C_2H_5O_2+CH_3O_2}$ (or $k_{C_2H_5O_2+CH_3CHO}$). Combined with the uncertainties ascribed to the acetylperoxy self-reaction and methylperoxy cross reaction, the net error in k_6 is again found to lie in the range 20−40%.

Figure 5 displays the temperature dependence of the $CH_3C(O)O_2 + C_2H_5O_2$ rate constant. Within the experimental errors, this rate constant is well fit by the Arrhenius expression

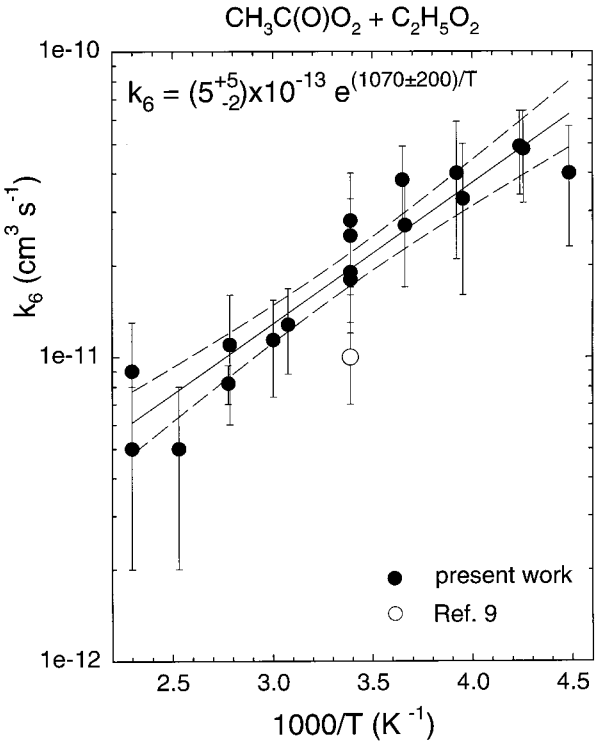

Figure 5. Temperature dependence of the $CH_3C(O)O_2 + C_2H_5O_2$ rate constant. Solid line is the best regression. Dashed lines represent 95% confidence limits for the regression.

$$k_6 = (5^{+5}_{-2}) \times 10^{-13}\, e^{(1070\pm200)/T}\ cm^3\ s^{-1} \qquad (12)$$

It exhibits a negative temperature dependence, as found for the acetylperoxy self-reaction and its cross reactions with CH_3O_2 and HO_2.[6,8] The error bars in the A-factor and activation energy are $\pm 2\sigma$, as determined statistically from the linear least-squares fit of $\ln(k_6)$ to $1/T$. The dashed lines in Figure 5 display the 95% confidence limits for the regression. Because measurement noise represents the largest source of error, and because the regression effectively "averages out" the random noise, these regression limits are tighter than the errors for the individual rate constant determinations.

IV. Discussion

The present rate constant determination for the acetylperoxy reaction with ethylperoxy radicals is in reasonable, though not *very* good, agreement with the room-temperature value reported by Villenave and Lesclaux.[9] The room-temperature rate constant of 2.0×10^{-11} cm^3 s^{-1}, based on the Arrhenius fit to our entire data set, is twice the previously reported value. Villenave and Lesclaux[9] relied on UV absorbance versus time traces recorded at the single wavelength of 235 nm to determine the rate constant. Because $CH_3C(O)O_2$, $C_2H_5O_2$, and CH_3O_2 all absorb at this wavelength, and considering the influence of secondary chemistry on the long-time decay of the $C_2H_5O_2$ and CH_3O_2 radicals just described, it would be difficult to ensure the accuracy of a rate constant determination based on a single wavelength. Thus, the earlier value of k_6 could be considered semiquantitative and, in that spirit, consistent with the present work.

Temperature-dependent rate constants are now available for four $CH_3C(O)O_2 + RO_2$ reactions, with R = H, CH_3, C_2H_5, and CH_3CO. These data are compared in Figure 6. All four

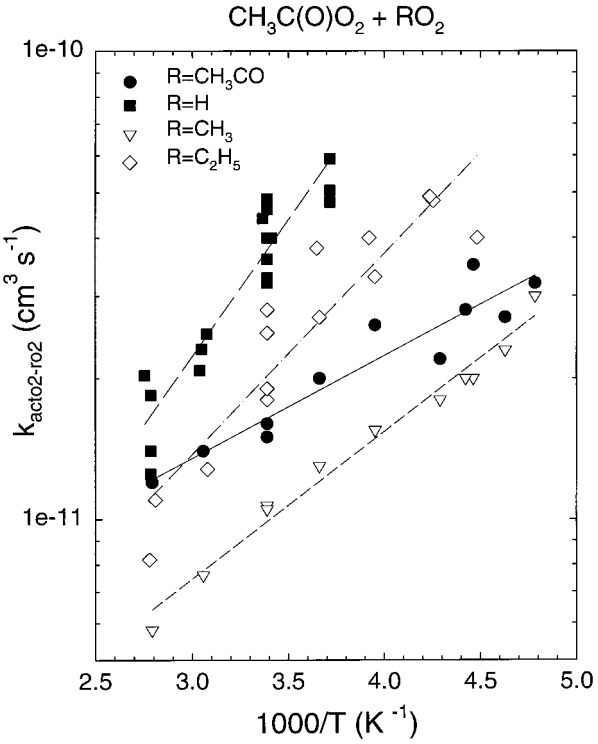

Figure 6. Comparison of the temperature-dependent rate constants for the reactions of acetylperoxy radicals with a variety of other peroxy radicals.

rate constants are relatively fast for peroxy−peroxy reactions, ranging at 295 K from 1×10^{-11} cm^3 s^{-1} for the methylperoxy reaction to 4×10^{-11} cm^3 s^{-1} for the reaction with HO_2. All exhibit a negative temperature dependence with apparent activation energies ranging from −500 K for the self-reaction to −1350 K for the HO_2 reaction.

The model study by Stockwell et al.[1] to investigate the importance of acetylperoxy−peroxy chemistry on the nighttime PAN and ozone levels utilized the Regional Acid Deposition Model (RADM2) atmospheric chemical mechanism. Stockwell et al.[15] subsequently refined this model to the Regional Atmospheric Chemistry Model (RACM), including, among other things, updated information regarding the acetylperoxy chemistry. However, the new kinetic data for the acetylperoxy radical was sparse; thus, Villenave et al.[4] recently measured room-temperature rate constants for a variety of $CH_3C(O)O_2 + RO_2$ rate constants and proposed to set the rate constant for this class of reactions to 1.0×10^{-11} cm^3 s^{-1}. In effect, this suggestion raised the previously used rate constants by a factor of 2−4. As a result, box model simulations under low NO_x, high volatile organic compound (VOC) conditions showed the $CH_3C(O)O_2 + RO_2$ reactions to account for 20% of the acetylperoxy loss. PAN levels were predicted to be 4% lower than those based on the original RACM.

The present work and our previous studies of acetylperoxy kinetics add two points to this discussion. First, the room-temperature rate constant of 1.0×10^{-11} cm^3 s^{-1} recommended to represent the acetylperoxy−organic peroxy class of reactions might be somewhat low; although based in Figure 6, which exhibits a range of $(1-2) \times 10^{-11}$ cm^3 s^{-1} at 295 K (omitting the HO_2 reaction), the suggested value is not far off. More important is the question of temperature dependence. The RACM assigns an apparent activation energy of −211 K to the $CH_3C(O)O_2 + C_2H_5O_2$ rate constant. For the acetylperoxy reactions with C3, C5, and C8 alkylperoxy radicals, the temperature dependence is made progressively steeper, with activation energies of −460, −522, and −683 K, respectively. Yet, the present experiments suggests that the $CH_3C(O)O_2 + C_2H_5O_2$ reaction rate constant exhibits an apparent activation energy of −1070 K. Thus, although a global $CH_3C(O)O_2 + RO_2$ rate constant of 1.0×10^{-11} cm^3 s^{-1} might serve well at 295 K, it could underestimate the rate constant by a factor of 2−3 at 270 K. The question of an appropriate temperature dependence for the kinetics of the acetylperoxy−organic peroxy class of reactions remains to be answered by additional, temperature-dependent kinetics measurements.

References and Notes

(1) Stockwell, W. R.; Milford, J. B.; Gao, D.; Yang, Y.-J. *Atmos. Environ.* **1995**, *9*, 1591.
(2) Shepson, P. B.; Hastie, D. R.; So, K. W.; Schiff, H. I.; Wong, P. *Atmos. Environ.* **1992**, *26A*, 1259.
(3) Hartsell, B. E.; Aneja, V. P.; Lonneman, W. A. *J. Geophys. Res.* **1994**, *99*, 21033.
(4) Villenave, E.; Lesclaux, R.; Seefeld, S.; Stockwell, W. R. *J. Geophys. Rev.* **1998**, *103*, 25273.
(5) Moortgat, G.; Veyret, B.; Lesclaux, R. *J. Phys. Chem.* **1989**, *93*, 2362.
(6) Maricq, M. M.; Szente, J. J. *J. Phys. Chem.* **1996**, *100*, 4507.
(7) Moortgat, G. K.; Veyret, B.; Lesclaux, R. *Chem. Phys. Lett.* **1989**, *160*, 443.
(8) Crawford, M. A.; Wallington, T. J.; Szente, J. J.; Maricq, M. M.; Francisco, J. S. *J. Phys. Chem.* **1999**, *103*, 365.
(9) Villenave, E.; Lesclaux, R. *J. Phys. Chem.* **1996**, *100*, 14372.
(10) Bridier, I.; Veyret, B.; Lesclaux, R.; Jenkin, M. E. *J. Chem. Soc., Faraday Trans.* **1993**, *89*, 2993.
(11) Maricq, M. M.; Wallington, T. J. *J. Phys. Chem.* **1992**, *96*, 986.
(12) Lightfoot, P. D.; Cox, R. A.; Crowley, J. N.; Destriau, M.; Hayman, G. D.; Jenkin, M. E.; Moorgat, G. K.; Zabel, F. *Atmos. Environ.* **1992**, *26A*, 1805.
(13) DeMore, W. B.; Sander, S. P.; Golden, D. M.; Hampson, R. F.; Kurylo, M. J.; Howard, C. J.; Ravishankara, A. R.; Kolb, C. E.; Molina, M. J. *Chemical Kinetics and Photochemical Data for Use in Stratospheric Modeling*; JPL, Publication 97-4, Pasadena, CA 1997.
(14) Delcroix et al. CMD meeting, Zurich, 1997.
(15) Stockwell, W. R.; Kirchner, F.; Kuhn, M. *J. Geophys. Rev.* **1997**, *102*, 25847.